

Study of the three-dimensional orientation of the labrum: its relations with the osseous acetabular rim

Noémie Bonneau,¹ July Bouhallier,² Michel Baylac,³ Christine Tardieu¹ and Olivier Gagey^{4,5}

¹UMR 7179 CNRS-Muséum National d'Histoire Naturelle, Paris, France

²UMR 7206 CNRS-Muséum National d'Histoire Naturelle, Paris, France

³UMR 7205 CNRS-Muséum National d'Histoire Naturelle, Paris, France

⁴Bicêtre University Hospital, Paris, France

⁵JE 2494 University Paris-Sud Orsay, Paris, France

Abstract

Understanding the three-dimensional orientation of the coxo-femoral joint remains a challenge as an accurate three-dimensional orientation ensure an efficient bipedal gait and posture. The quantification of the orientation of the acetabulum can be performed using the three-dimensional axis perpendicular to the plane that passes along the edge of the acetabular rim. However, the acetabular rim is not regular as an important indentation in the anterior rim was observed. An innovative cadaver study of the labrum was developed to shed light on the proper quantification of the three-dimensional orientation of the acetabulum. Dissections on 17 non-embalmed corpses were performed. Our results suggest that the acetabular rim is better represented by an anterior plane and a posterior plane rather than a single plane along the entire rim as it is currently assumed. The development of the socket from the Y-shaped cartilage was suggested to explain the different orientations in these anterior and posterior planes. The labrum forms a plane that takes an orientation in between the anterior and posterior parts of the acetabular rim, filling up inequalities of the bony rim. The vectors V_L , V_{A2} and V_P , representing the three-dimensional orientation of the labrum, the anterior rim and the posterior rim, are situated in a unique plane that appears biomechanically dependent. The three-dimensional orientation of the acetabulum is a fundamental parameter to understand the hip joint mechanism. Important applications for hip surgery and rehabilitation, as well as for physical anthropology, were discussed.

Key words: acetabulum; biomechanics; bipedal gait; hip joint; total hip arthroplasty.

Introduction

The exclusive bipedal locomotion of humans implies strong mechanical constraints on the coxo-femoral joint, especially during the one-legged stance. Both stability and mobility are required from the hip joint to ensure a functional interface between the pelvis and lower limbs. Precise knowledge of the hip joint has important clinical implications in hip surgery and rehabilitation, as well as for physical anthropology as it improves biomechanical understanding of this complex joint from an evolutionary viewpoint. Understanding the

three-dimensional orientation of the coxo-femoral joint remains a challenge as it is fundamental to ensure an efficient bipedal gait and posture. The anteversion and inclination angles are currently used to quantify the orientation of the acetabulum (Lewinnek et al. 1978; Murray, 1993; Lazennec & Saillant, 2004; Lazennec et al. 2004; Tardieu et al. 2006, 2008). However, several problems concerning these angles can be pointed out. According to the disciplines, different reference planes are used to describe the position of the pelvis leading to different definitions of the anteversion and inclination angles (Murray, 1993). Most important, the available method to quantify the orientation of the acetabulum uses parameters defined in two dimensions instead of a three-dimensional axis, which would be more informative.

The three-dimensional orientation of the acetabular axis is defined as the perpendicular to the plane that passes along the edge of the acetabular rim (Calandruccio, 1987). A regression plane computed from the acetabular rim edge would provide a direction vector corresponding to the three-dimensional orientation of the acetabular axis.

Correspondence

Noémie Bonneau, UMR 7179 CNRS-MNHN – Mécanismes adaptatifs: des organismes aux communautés, Muséum National d'Histoire Naturelle, 57 rue Cuvier, Pavillon d'Anatomie Comparée, C.P. 55, 75231 Paris Cedex 05, France. T: 00 33 (0)1 40 79 57 14; E: nbonneau@mnhn.fr

Accepted for publication 27 January 2012

Article published online 23 February 2012

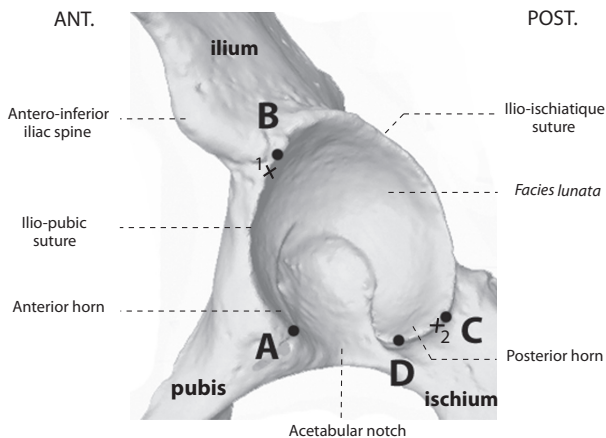


Fig. 1 Lateral view of a left acetabulum. The anterior and posterior horn tips are indicated by the letters A and D. Along the rim two inflexions can be systematically identified: B represents the most cranial inflexion where the indentation of the anterior part of the rim appears; C, the most caudal inflexion, was placed at the beginning of the curvature of the posterior horn. B and C allow the division of the rim in two parts named the anterior and posterior acetabular rims. The landmarks 1 and 2 (indicated by crosses) correspond to the insertion of the ilium and the ischium on the acetabular rim.

However, the acetabular rim is not regular as an important indentation in the anterior acetabular rim was observed (Fig. 1; Fabeck et al. 1998, 1999; Maruyama et al. 2001; Vandebussche et al. 2007, 2008). The irregular shape of the acetabular rim implies that the three-dimensional orientation of the acetabulum, and by consequence the anteversion and inclination angles calculated from it, changes according to the point used to compute the regression plane (Fabeck et al. 1998; Thompson et al. 2000; Lazennec & Saillant, 2004; Zilber et al. 2004). Consequently, the method based on a single plane appears inappropriate to model the entire acetabular rim.

Currently, only the bony limits of the acetabulum are used to determine its orientation. The three-dimensional orientation of the acetabulum and the irregular nature of the acetabular rim were explored in this study using the three-dimensional anatomy of the labrum. The labrum is a continuous fibrocartilage, with dense connective tissue at its external circumference (Shibutani, 1988; Petersen et al. 2003), attached along the whole acetabular rim and the transverse ligament over passing the acetabular notch (Seldes et al. 2001; Tan et al. 2001; Petersen et al. 2003; Lewis & Sahrman, 2006). It forms a complete circle filling up inequalities of the bony rim. The function of the acetabular labrum is complex. It deepens the socket and acts like a sealant resulting in a vacuum phenomenon, thus providing further stability (Takechi et al. 1982; Ferguson et al. 2000a, 2003). Moreover, it manages a transition between the hard acetabular rim and the soft articular capsule ensuring a progressive transmission of the forces during hip loading (Ferguson et al. 2000b).

In this paper an innovative cadaver study of the three-dimensional anatomy of the labrum was developed to analyse its relationships with the acetabular rim. Developmental and biomechanical interpretations were investigated, and clinical and anthropological implications were suggested.

Materials and methods

Materials

After approval of the protocol by the scientific committee of the 'Centre du Don des Corps' (University of Paris Descartes, France), dissections were performed on 17 non-embalmed cadavers (nine men and eight women) with a mean age of 75.2 years (SD = 12.8 years; range 56–93 years). Three hips either with scars or evidence of osteoarthritis were rejected, thus 31 hips were studied.

Dissection protocol

The pelvi-femoral complex was removed from all corpses between the third lumbar vertebra and the tibio-femoral joint. Soft tissues were cut away. At the coxo-femoral joint the articular capsule was cut and the femoral head was removed from the acetabular cavity while taking care to avoid damage to the labrum. An anatomical preparation with an intact labrum was obtained. Four stainless-steel nails with a diameter of 1 mm were implanted in each hip bone in order to generate a three-dimensional system of reference landmarks. The bone was pierced by means of a 0.9-mm-diameter drill and stainless-steel nails were placed in the holes. The nails were implanted, on the one hand, with a maximal dispersion relative to the overall pelvic volume to produce an accurate three-dimensional system and, on the other hand, in the thickest parts of the bones, for example the iliac tubercle and the pelvic brim, to avoid their disassembly during the study period.

Digitalisations were performed using a MicroScribe® G2 (Immersion, France) with a precision of ± 0.38 mm according to the constructor. Three-dimensional coordinates (x , y , z) were recorded in a millimetric orthonormal reference system.

For each hip bone, the pelvis was immobilised in a clamp and the coordinates of the four nails (reference landmarks) were digitised in the centre of the nail head. The apex of the labrum, i.e. its free margin, was acquired by recording coordinates of successive points (Fig. 2A) using the MicroScribe programmed to take coordinates 1 mm apart. These acquisitions had to be done shortly after the opening of the articular capsule to prevent desiccation of the labrum, which would cause the loss of its natural shape.

To test the intra- and inter-observer measurement errors, this digitising protocol was repeated six times by one observer and three times by a second observer on eight acetabula.

Osteological treatments

After dissections the pelvis were collected and cleaned by osteological treatments performed by the technician of the SPOT (Service de Préparations Ostéologiques et Taxidermiques) of the National Museum of Natural History of Paris (France). The osteological preparation consisted of different baths of

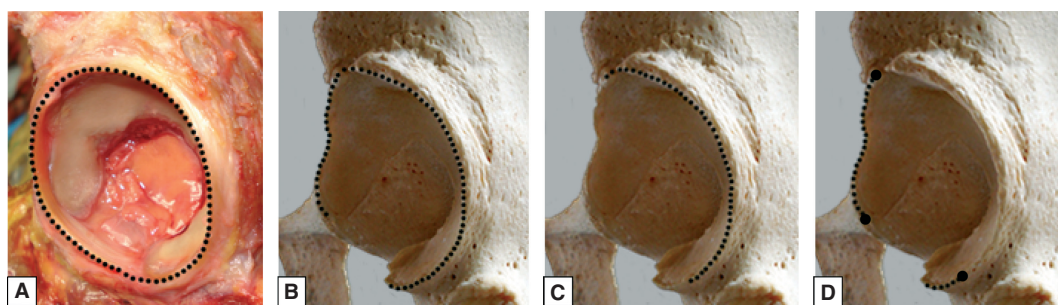


Fig. 2 Successive points 1 mm apart were digitised along (A) the intact labrum, (B) the totality of the acetabular rim, (C) the posterior part of the acetabular rim and (D) the anterior part of the acetabular rim. With these data four planes named, respectively, P_L , P_T , P_A and P_P combined with their respective direction vector V_L , V_T , V_A and V_P were obtained. Due to a methodological problem (see text), the anterior rim was modelled using a regression plane P_{A2} based on points A, B and C (large points in D) resulting in a vector V_{A2} .

alcohol, enzymatic digestion and drying. These treatments did not affect the nails position. To test for potential bone deformation induced by osteological preparation, the six Euclidian distances between the four nails of each hip bone were computed and compared before and after preparation. Given a precision of the Microscribe® G2 at 0.38 mm and a nail diameter of 1 mm, we fixed the threshold for error due to protocol-induced measurement error at twice the instrument precision, i.e. 0.76 mm. Differences between distances obtained on isolated bones before and after preparation never reached 0.76 mm, implying no bone deformation during osteological preparations.

Data collection on dry bones

On dry bones, a new anatomical description of the acetabular rim was performed. The acetabular rim, interrupted by the acetabular notch, is limited by the anterior and posterior horn tips (indicated, respectively, by A and D in Fig. 1). Two inflexions were systematically identified: a most cranial inflexion (Fabeck et al. 1998), where the indentation of the anterior part of the rim appears (B in Fig. 1); and a most caudal inflexion, which was placed at the beginning of the posterior horn curve (C in Fig. 1). They were used to divide the acetabular rim in two parts, named anterior and posterior acetabular rims.

New data acquisitions were performed on osteological specimens. The hip bone was immobilised in a clamp and the three-dimensional coordinates of the four nails were recorded.

Successive points, using the MicroScribe programmed to take coordinates 1 mm apart, were digitised along the totality of the acetabular rim (from A to D in Fig. 1, resulting in Fig. 2B), along its posterior part only (from B to C resulting in Fig. 2C), and along its anterior part only (from A to B and from C to D resulting in Fig. 2D). Successive points were also acquired along the edges of the *facies lunata*, the articular surface of the acetabulum taking a characteristic horseshoe shape. Finally, the three-dimensional coordinates of the homologous landmarks corresponding to the anatomical points A–D (Fig. 1) were recorded, as well as the two landmarks corresponding to the insertion of the ilium and the ichium on the acetabular rim (respectively, 1 and 2 in Fig. 1).

The digitising protocol was repeated six times by one observer and three times by a second observer on eight acetabula to test intra- and inter-observer errors.

Superimposition of data acquired on fresh cadavers and data acquired on dry bones

To study the orientation of the labrum compared with the acetabular rim, a first step of superimposition was required in order to have the data recorded on cadavers and the data recorded on dry bones represented into a same three-dimensional space. The superimposition process based on a Generalised Procrustes Analysis (Gower, 1975; Rohlf & Slice, 1990) corresponds to a scaling step followed by translations and rigid three-dimensional rotations of the bones, using the landmarks defined by the four nails. The different outlines followed passively the translation and rotations calculated using the nail coordinates. The centroid size of the nails used during the scaling step was restored before further mathematical and statistical treatments because it has no biological meaning. The use of the nails guarantees reference landmarks with equal and spherical variance, and the location of the nails was uncorrelated (Richtsmeier et al. 2005). A custom-designed function of the Rmorph library for R (Baylac, 2010) was used for this superimposition process.

Data processing

All analyses were performed using the R graphical and statistical package v.2.9.0 (R Development Core Team, 2009).

Regression planes, using the least squares method, were computed based on the points acquired on the entire dry acetabular rim (Fig. 2B), on the posterior rim only (Fig. 2C) and on the anterior rim only (Fig. 2D), resulting in three planes ($a_i x + b_i y + c_i z + d_i = 0$), which were named, respectively, P_T (total plane), P_P (posterior plane) and P_A (anterior plane). For each plane, the standard deviation (SD), i.e. the mean of the distance of each point from the regression plane, was computed. A Flinger–Killeen test was computed to compare the values of the standard deviation obtained based on P_T and the mean value of the standard deviations obtained based on the two planes P_P and P_A .

The regression plane based on the points acquired on the labrum (Fig. 2A) was computed, resulting in the plane P_L (labrum plane). In summary, we obtained four planes P_T , P_P , P_A and P_L combined with their respective direction vector (a_i , b_i , c_i) named V_T , V_P , V_A and V_L . A methodological problem in the reconstruction of the vector V_A was observed. To obtain more accurate data, we decided to reconstruct the plane of the anterior rim using a regression based on the three points A–C (large

points in Fig. 2D) rather than on the successive points acquired on the anterior part of the acetabular rim. This methodological choice is described and explained in the discussion. A new plane P_{A2} was thus calculated combined with its direction vector V_{A2} .

To evaluate the intra- and inter-observer measurement errors, the regression planes were computed on each repetition performed by the first and second observers on eight acetabula. A mean vector of the six direction vectors obtained by the first observer and a mean vector of the three direction vectors obtained by the second observer were calculated. The intra-observer measurement error corresponds to the mean angle between the mean vector obtained by the first observer and each direction vector of his six repetitions. The inter-observer measurement error corresponds to the angle between the mean vector obtained by the first observer and the mean vector obtained by the second observer.

To analyse the different three-dimensional orientations of the labrum and the posterior and anterior rims, the angles between V_L , V_{A2} and V_P were computed for each acetabulum. First, both linear least squared regressions and correlation tests, using the Pearson method, were calculated on the different angles. Moreover, ANOVAS were performed to test the laterality, sex and age effects on the three angles. These three angles are interdependent, requiring the Bonferroni correction. Second, the coplanarity of the vectors V_L , V_{A2} and V_P was tested. The three angles between these vectors served to compute the percentages of the two smaller angles in comparison with the greater angle. If the sum of these two percentages equalled to 100%, the coplanarity of the three vectors was concluded and a new plane P_C (convergence plane) was established combined with its direction vector V_C .

The mean height of the labrum and the acetabular rim in relation to the acetabular centre were also analysed. A regression sphere computed based on the points acquired on the edge of the *facies lunata* served to obtain the coordinates of the acetabular centre O. This point O was projected, first, in P_L and, second, in P_T , allowing to obtain the mean height of the labrum and the acetabular rim in relation with the acetabular centre. A negative value was attributed when the plane passed below O, a positive value when the plane passed above O. Correlation tests were performed between these two heights and, first, the orientation of V_L , V_{A2} and V_P and, second, the age.

The three-dimensional orientation of P_C was explored in relation with the more general anatomy of the acetabular region. The two landmarks acquired at the intersection between the acetabular rim and, first, the ilium (landmark 1 in Fig. 1) and, second, the ischium (landmark 2 in Fig. 1) served to compute

the axis (D). Moreover, the vector OA between the acetabular centre and the point A was calculated. Both the angle between V_C and (D) and the angle between V_C and OA served to analyse the orientation of P_C in the acetabular region. ANOVAS were performed to test the laterality, sex and age effects on the orientation of P_C .

Results

On average, the standard deviation calculated based on P_T was greater than the ones calculated based on P_A and P_P (Table 1). The planes P_A and P_P provided a significantly smaller standard deviation than the plane P_T according to the Fligner–Killeen test (med $\chi^2 = 6.6$, $P = 0.010$, $N = 31$). According to these results, the anterior and posterior parts of the acetabular rim are better represented separately than by the plane of the total rim. Thus, the description of the acetabular orientation using the two planes P_A and P_P appears more accurate than using a single plane P_T .

There is a good reliability in the determination of the direction vector V_L , V_T , V_P and V_{A2} . The intra-observer measurement errors were, in all cases, inferior to 0.9° . The maximal inter-observer measurement error was 1.7° , corresponding to the error in the determination of V_{A2} .

The angle formed by V_{A2} and V_P was 21.4° on average (SD = 8.6° ; range = 9.8° – 41.0°), corresponding to a mean angle of 158.6° between P_{A2} and P_P (Fig. 3). There were significant effects of sex and age on this angle (Table 2). The mean angle formed by V_A and V_P was 24.3° in females

Table 1 Mean maximal and minimal values of the standard deviation (SD) computed based on the planes P_T , P_P and P_A .

	Standard deviation (mm)		
	Mean	Maximal	Minimal
Total rim (P_T)	2.1	3.6	1.5
Posterior rim (P_P)	0.8	2.0	0.4
Anterior rim (P_A)	1.3	2.6	0.7

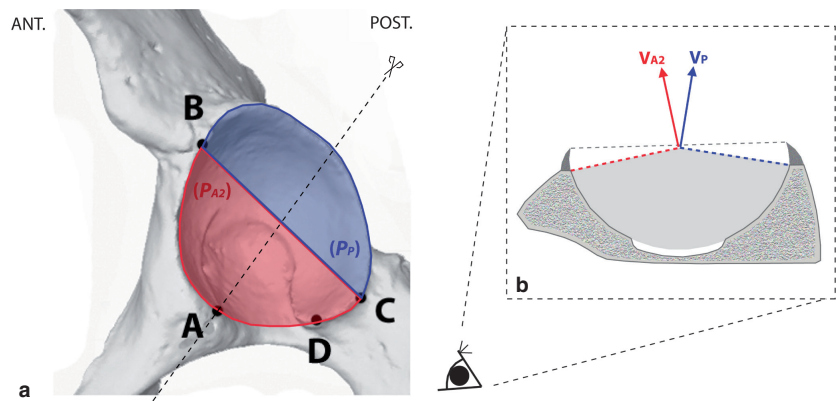


Fig. 3 The planes P_{A2} and P_P , computed using the anterior and posterior acetabular rims, are not in the same plane but they formed a mean angle of 158.6° . (a) A general view illustrating the plane P_{A2} of the anterior rim (in red) and the plane P_P of the posterior rim (in blue). A transversal slice was observed along the dotted line and present in (b). (b) The vector V_{A2} (red dotted line) and V_P (blue dotted line) form a mean angle of 21.4° . The plane of the labrum is represented by the grey dotted line.

Table 2 Results of the ANOVA performed on the three angles between V_L , V_{A2} and V_P to test the age, sex and laterality effects.

	$V_{A2} - V_P$		$V_L - V_{A2}$		$V_L - V_P$	
	<i>F</i>	<i>P</i>	<i>F</i>	<i>P</i>	<i>F</i>	<i>P</i>
Age	5.9	0.019*	3.44	0.076 NS	4.78	0.02*
Sex	6.77	0.02*	9.34	0.0055*	1.69	0.21 NS
Laterality	0.39	0.92 NS	0.002	0.96 NS	0.0075	0.94 NS
Age × sex	0.91	0.35 NS	0.6	0.45 NS	1.11	0.3 NS
Age × laterality	0.16	0.69 NS	0.7	0.41 NS	0.022	0.88 NS
Sex × laterality	0.034	0.86 NS	0.37	0.55 NS	0.18	0.68 NS
Age × sex × laterality	3.8	0.064 NS	2.56	0.13 NS	2.59	0.12 NS

Significance levels according to the Bonferroni correction. NS, not significant.

*Significant at 0.02; **significant at 0.003; ***significant at 0.003.

and 18.8° in males, and tended to decrease with age in both males and females. There is no significant effect of the side (left vs. right).

The orientation of V_L in relation to V_{A2} and V_P was explored. On average, a coplanarity of these three vectors was concluded because the sum of the percentages of the angles $V_L V_{A2}$ and $V_L V_P$ compared with angle $V_{A2} V_P$ equalled 103.7% across the 31 acetabula. In summary, the vectors V_P , V_L and V_{A2} were aligned in a same plane. The greater the angle $V_{A2} V_P$ was, the better the vectors V_L , V_P and V_{A2} were aligned (correlation between the angle $V_{A2} V_P$ and the sum of the percentages: $r_{\text{Pearson}} = -0.39$; $P = 0.029$; $N = 31$). In P_C , the variable relationship between these three vectors can be described by the significant positive correlation computed between the angles $V_A V_P$ and $V_L V_A$ ($r_{\text{Pearson}} = 0.83$; $P < 0.0001$; $N = 31$; Fig. 4a). In Fig. 4b, two extreme cases, i.e. with a minimal and maximal value of the angle between V_{A2} and V_P , are represented. The vector V_L was closer to V_{A2} than V_P on average, i.e. the labrum was higher in the posterior part than in the anterior part, and tended to be in an average position between V_{A2} and V_P for small values of the angle $V_{A2} V_P$. Using the equation $y = 0.42x - 0.46$ based on the linear regression, it is possible to estimate the angle $V_L V_{A2}$ using the value of the angle $V_{A2} V_P$. Based on this equation, the angle $V_L V_{A2}$ is predicted using the real angle $V_{A2} V_P$ with an error of 1.7° on average (SD = 1.1°; range = 0.1°–3.8°). There was a significant effect of age on the angle $V_L V_P$ and a significant effect of sex on the angle $V_L V_{A2}$ (Table 2).

Across the 31 acetabula, the mean height of the labrum relative to the acetabular centre O was +1.7 mm (SD = 2.33 mm; range = -2.7 mm to +6.7 mm). The mean height of the acetabular rim was -3.2 mm (SD = 2.5 mm; range = -6.9 mm to +3.3 mm). No correlation was detected between these two heights and the orientations of V_L , V_A and V_P . There is a significant effect of age on the height of the acetabular rim ($r_{\text{Pearson}} = 0.38$; $P = 0.035$; $N = 31$).

On average, the plane P_C was aligned with the vector OA and perpendicular to the axis (D). The mean angle between

V_C and (D) equalled 8.1° (SD = 4.9°; range = 0.4°–18.5°). There was a significant correlation between the angle $V_{A2} V_P$ and the angle between V_C and (D) ($r_{\text{Pearson}} = -0.47$; $P = 0.008$; $N = 31$). The mean angle between V_C and OA equalled 83.8° (SD = 4.9°; range = 75.4°–89.9°).

Discussion

This study provides a new anatomical description of the acetabular region, and provides insights regarding the three-dimensional anatomy of the acetabular rim in relation to the intact labrum.

The Y-shaped cartilage, a suggested source of the irregular acetabular rim

This study confirms the irregularity of the acetabular rim already demonstrated in the literature (Fabeck et al. 1999; Maruyama et al. 2001; Zilber et al. 2004; Vandebussche et al. 2008). An anatomical examination of dry bones has shown that the acetabular rim can be divided in an anterior and a posterior part (Fig. 1). Two planes (P_A and P_P) were computed based on these two parts, and the results provide evidence that they are better represented by separate planes than the unique one computed based on the entire rim (P_T) generally used to determine the acetabular orientation. Thus, rather than to form an angle of 180° as it is currently assumed, the posterior and anterior parts of the acetabular rim form an angle of 158.6° on average.

This angle could have implications for the mobility of the femur. Indeed, the femoral neck is pushed onto the acetabular rim less rapidly with a greater angle $V_{A2} V_P$ than with a smaller one. This hypothesis is supported by the observed correlation between the greater angles $V_{A2} V_P$ and $V_L V_{A2}$ observed in females and their general greater femoral range of motion compared with males.

This irregularity in the morphology of the acetabular rim could be explained by the different origins of the anterior and posterior parts of the acetabular rim. The growth of

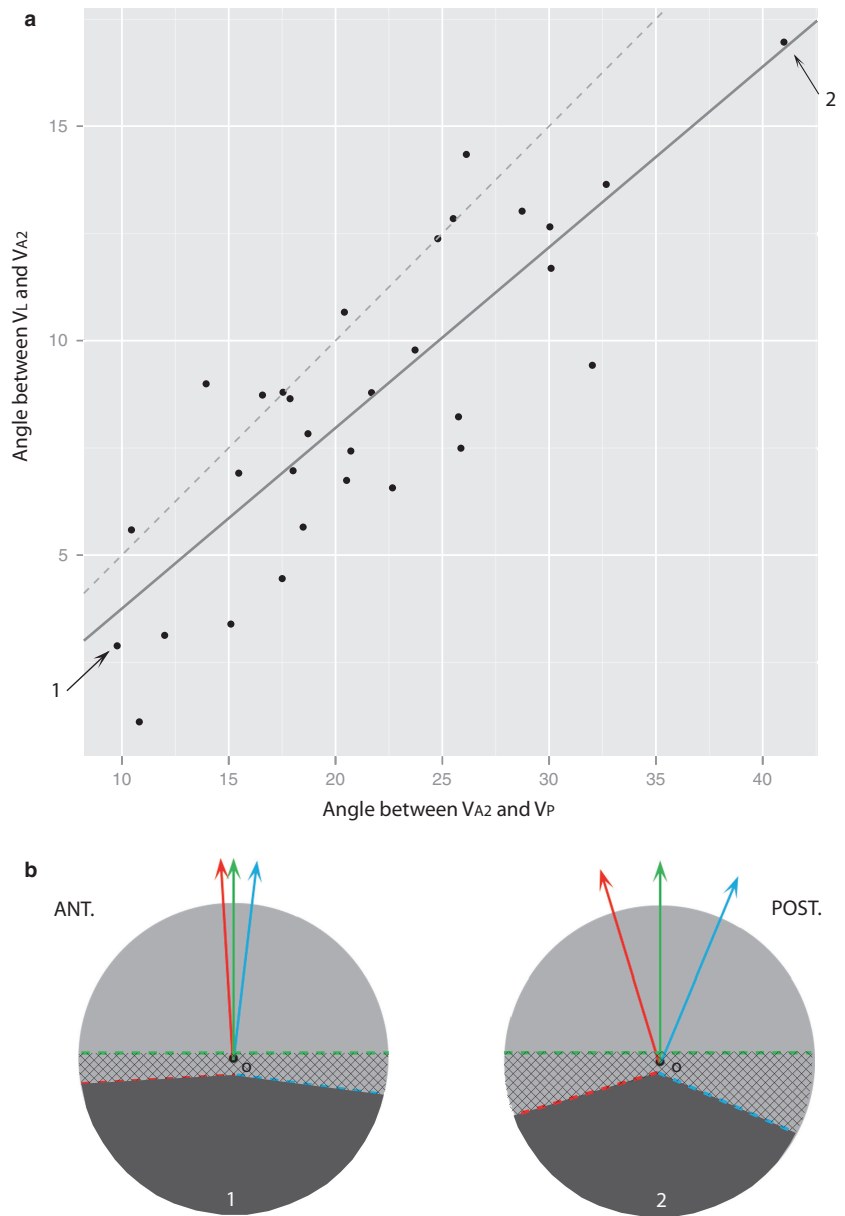


Fig. 4 (a) There is a significant positive correlation between the angle $V_A V_P$ and the angle $V_L V_A$ ($r_{\text{Pearson}} = 0.83$; $P < 0.0001$; $N = 31$), which is represented in the graph by a regression line (grey solid line). The light grey dotted line represents shapes for which V_L would be exactly at the middle of V_{A2} and V_P . A comparison between the two lines shows that V_L is generally closer to V_{A2} than V_P , and that V_L is near to an intermediate position between V_{A2} and V_P when the angle $V_{A2} V_P$ decreases. (b) Two cases were represented to illustrate the changes of the relationships between V_A (in red), V_P (in blue) and V_L (in green) when the angle $V_{A2} V_P$ takes its minimal or maximal value (individuals 1 and 2, respectively, marked by arrows in a). These two cases are viewed in the plane of the three vectors V_L , V_{A2} and V_P , i.e. at the perpendicular to P_C . The hatched areas illustrate the height of the labrum in its anterior and posterior parts.

the acetabular socket is derived from a Y-shaped cartilage composed by the ilio-pubic, ilio-ischiatic and ischio-pubic branches. The posterior part grows from the ilio-ischiatic branch, while the anterior part is formed by both the ilio-pubic and ischio-pubic branches. Each branch of the Y cartilage is submitted to different mechanical constraints resulting in growth in a different direction (Fig. 5). In reality, the anterior part of the acetabular rim should be divided in two parts: the superior and the inferior part whose growths are, respectively, governed by the ilio-pubic branch and the ischio-pubic branch. However, because of the acetabular notch, it is impossible to reconstruct an orientation of the antero-inferior part. Thus, to obtain a mean orientation of the anterior part, and not to have a vector disproportionately influenced by the superior part, we

chose to determine the orientation of the anterior part of the acetabular rim based on the three points A–C, resulting in V_{A2} , rather than successive points acquired along the anterior rim.

Three-dimensional orientation of the anterior and posterior acetabular rims compared with the intact labrum

The three-dimensional orientations of the anterior and posterior planes were explored in relation with the morphology of the labrum. The present results provide evidence that the three vectors V_L , V_{A2} and V_P are coplanar, i.e. they are situated in a unique plane P_C . The position of the vector V_L can be described in relation to V_{A2} and V_P when they lie

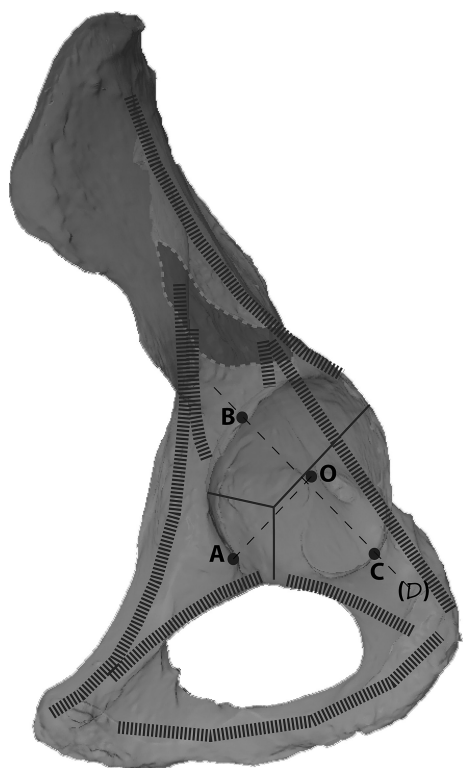


Fig. 5 The irregularity in the morphology of the acetabular rim can be explained by the Y-shape of the growth cartilage (solid lines). The posterior part grows from the ilio-ischiatic branch, while the anterior part is formed by the ilio-pubic and ischio-pubic branches. Each branch of the Y cartilage is not submitted to the same constraints, resulting in growth in a different direction. The acetabulum is integrated in the complex biomechanical system of the hip bone. The acetabulum is surrounded by a network of different trabecular systems (thick dotted lines), which is load history dependent. A link between the orientation of the plane P_C and the biomechanical loading context was identified. The points A–C, which correspond more generally to the intersection of the pubis, ilium and ischium with the acetabular rim, are located in the area of the transition between the different trabeculae, i.e. in the least constrained area. Our results showed that the plane P_C is precisely aligned with the axis formed by B and C (thin dotted line) and perpendicular to the axis formed by O and A (thin dotted line), suggesting an effect of biomechanical loading on the orientation of P_C . The scan of this left hip bone was performed using a Breuckmann® surface scanner and the view was chosen to display concurrently the anterior and posterior networks of the trabecular system, the sacroiliac joint from which they emerge, and to illustrate that A–C correspond to areas of transition between the different trabeculae.

in the plane P_C . As illustrated in Fig. 4, V_L lies closer to V_{A2} than to V_P . This result is consistent with the general assertion that the labrum is higher in its posterior part than in its anterior part (Seldes et al. 2001; Lewis & Sahrman, 2006). The orientation of P_C was explored relative to the general anatomy of the acetabular region. On average, this plane is, on the one hand, parallel to the vector formed by the acetabular centre O and the anterior horn tip of the *facies lunata* (landmark A in Fig. 1) and, on the other hand, per-

pendicular to the axis formed by the point of intersection of the ilium and the ischium on the acetabular rim (landmarks 1 and 2 in Fig. 1). In summary, the labrum forms a plane that takes an orientation inbetween the orientation of the posterior and anterior parts of the acetabular rim filling up inequalities of the bony rim. The three planes tilt along the axis formed by the intersection of the ilium and the ischium and the acetabular rim (BC), which is perpendicular to the axis formed by the acetabular centre and the anterior horn tip of the *facies lunata* (OA). It emerges from the acetabular rim, described previously as an irregular profile, a precise structure that can be described in the more general anatomy of the acetabulum.

Biomechanical investigations

The hip joint is a very complex structure, and its functional tasks in the support and transmission of the forces between the pelvis and lower limbs is well recognised. In a first approximation, this very stable diarthrosis could be considered as a perfect ball and socket joint. In reality, variations from this simplistic model have been described and implications in the amelioration of the acetabular biomechanics have been demonstrated. First, the general horseshoe-shaped structure of the *facies lunata* optimises the stress distribution along the contact surface and refocuses the peak of maximal constraints in the centre of the surface rather than close its edge (Daniel et al. 2005). More precisely, rather than a perfect sphere this surface corresponds to an arched dome (Bullough et al. 1968, 1973; Goodfellow & Mitsou, 1977). The compliance of acetabular bone and cartilage allows deformations of this arched dome undergoing high constraints, for example during the one-legged stance of the walking, resulting in an increase of the sphericity and a more homogeneous distribution of the forces along the total contact surface while maximal forces are focused on the acetabular roof without deformation (Dalstra & Huiskes, 1995). Moreover, this incongruity between the acetabular roof and the femoral head could ensure the circulation of synovial fluid needed for the nutrition and lubrication of the cartilage (Greenwald & O'Connor, 1971). Under low loads, for example during the swing phase of the walking, the femoral head contacts the acetabular surface in its antero- and postero-superior parts [zones 15 and 16 described by Byers et al. (1970)], leaving the acetabular roof unloaded. Under high loads, the acetabular roof [zone 17 according to the description of Byers et al. (1970)], composed by a different type of more elastic cartilage (Day et al. 1975), comes in contact with the femoral head involved in weight-bearing (Greenwald & Haynes, 1972; Day et al. 1975; Mizrahi et al. 1981). Furthermore, the horns of the *facies lunata* catch up with the femoral head until they touch it (Teinturier et al. 1984; Lazennec et al. 1997). The labrum, which deepens the socket, also plays an important role in the biomechanics of the coxo-femoral joint.

Indeed, it forms the sealing mechanisms that protect the cartilage layers (Takechi et al. 1982; Ferguson et al. 2003) and manage the transition between the osseous acetabular rim and the femoral neck. Finally, the acetabulum is integrated in the highly structured mechanical system of the hip (Dalstra & Huiskes, 1995). The acetabulum is surrounded by a very complex trabecular system that is load history dependent and, thus, reflects the locomotor behaviours (Macchiarelli et al. 1999, 2001; Martínón-Torres, 2003). Yet, the trabecular network is subjected to lower strains than the cortex shell (Dalstra & Huiskes, 1995). A link between the orientation of the plane P_C and the biomechanical context is identified here. The points A–C (Fig. 1), which correspond more generally to the intersection of the pubic, ilium and ischium with the acetabular rim, are located in the area of transition between the different trabeculae (Fig. 5), i.e. in a less constrained area. Our result showed that the plane P_C is precisely aligned with the axis formed by B and C and perpendicular to the axis formed by O and A, suggesting an effect of the biomechanical system on the orientation of P_C .

During ageing, the compliance of the acetabulum decreases resulting in an alteration of the acetabular biomechanics. The system becomes modified and many age-dependent changes can be observed (Goodfellow & Bullough, 1968; Bullough et al. 1973; Goodfellow & Mitsou, 1977; Teinturier et al. 1984). In our study, modifications in the acetabular rim profile related to the age of the subjects were also observed. The posterior part of the acetabular rim tends to move up, as illustrated by the significant decrease of the angle $V_L V_P$, resulting in a general decrease of the angle $V_{A2} V_P$ and a general increase of the height of the mean acetabular rim in relation to the acetabular centre. The vector V_L tends to be in an intermediate position between V_{A2} and V_P , rather than to be closer to V_{A2} as it is observed in younger subjects. In old persons the acetabular opening is quite planar. In these cases, there is an alteration of the coplanarity between V_{A2} , V_P , V_L and the plane P_C deviates from, on the one hand, its parallel orientation compared with the axis formed by the acetabular centre O and the anterior horn tip A and, on the other hand, its perpendicular orientation compared with the axis formed by the insertion of the ilium and the ischium on the acetabular rim. These changes are in accordance with the modifications in the trabecular systems of the hip bone observed during ageing (Teinturier et al. 1984).

Clinical and anthropological implications

An accurate orientation of the prosthetic cup during total hip arthroplasty (THA) is key to prevent conflicts between the femoral neck and the acetabular rim, which can induce hip dislocation (Lazennec et al. 2004; Rousseau et al. 2009). Thus, a precise knowledge of the acetabular orientation has important implications in the surgical domain and more precisely during hip surgery. For THA performed using com-

puter-assisted surgery, surgeons currently use the Lewinneck's plane as a reference to orient the implant (Lewinneck et al. 1978). This plane is described by the two anterior superior iliac spines and the pubic symphysis. These markers are hard to identify *in vivo* as the palpation of the iliac spines and the pubis is imprecise due to the smooth bony surface and the presence of soft tissues (Pinoit et al. 2007; Lee & Yoon, 2008). Moreover, even assuming that the reference plane was well identified, the values of anteversion and inclination proposed for the orientation of the cup are mean values based on radiographic studies for an entire population (Lewinneck et al. 1978) and are not calculated on a case by case basis. Being able to describe the acetabular orientation with three-dimensional parameters, independent of any reference plane and adapted to each patient, may contribute to improve and secure the final position of the cup in THA.

Our results show the important difference in the orientation of the anterior and posterior parts of the acetabular rim, which should not be neglected in THA. The analyses of the angle $V_{A2} V_P$ suggest the biomechanical role of this angle that could be important in the femoral mobility. The orientation of the labrum in balance between the posterior and the anterior plane, closer to the anterior plane, and the precise orientation of P_C in the acetabular biomechanics suggest that the irregularity in the acetabular rim has a functional meaning.

Based on the present results, it is possible to predict the three-dimensional orientation of the labrum (V_L) with high accuracy. Both the anterior and posterior rims are accessible during surgery or before using CT scanner data resulting in the possibility to calculate the two vectors V_{A2} and V_P . Based on these data the plane P_C can then be computed. The vector V_L should be placed in P_C . Finally, the predictive equation proposed in the Results section would provide the more likely orientation of V_L in relation to V_{A2} and V_P with an error of only 1.7° on average. However, there is no correlation between the height of the labrum or the height of the mean acetabular rim in relation to the acetabular centre and the orientation of V_L , V_{A2} and V_P . Thus, only mean values, respectively, $+1.7$ mm and -3.2 mm can be used.

The prediction of the orientation of the labrum can be an alternative method in the determination of the acetabular orientation. Indeed, the prosthetic cup presents a perfect plane between the anterior and posterior parts of the rim, and positioning of this cup using the orientation of the labrum could limit the conflicts between the femoral neck and the cup. However, our results show that the angle $V_{A2} V_P$ could have a biomechanical role and a cup with a simple opening plane may explain the conflicts between the anterior part of the cup and the femoral neck recognised when patients sit down. In a normal hip, the anterior indentation likely increases the mobility and avoids this conflict. Moreover, the indentation of the anterior part could also ensure

a smooth and proper functioning of the ilio-psoas muscle, while an angle of 180 ° could cause pain at the level of the ilio-psoas tendon, which passes along the anterior rim (Vandenbussche et al. 2008).

This anatomical description of the acetabular rim may also have implications in physical anthropology. The labrum, a soft tissue, is absent in fossils. The better understanding of the biomechanics of the acetabulum and the possibility to predict the orientation of the labrum can thus improve the understanding of the evolution of a bipedal gait and posture, an important issue in the study of human evolution.

Acknowledgements

We thank Mme Edith Bordereaux, the scientific responsible of the 'Centre du Don des Corps' and all the team of this institution for their help with this project. Special thanks for the osteological preparations to Eric Pellé. We thank Caroline Simonis for her great help in establishing the superimposition function. This paper benefited from the morphometric facility of the Paris Muséum (UMR 2700 CNRS – MNHN: 'Plateforme de Morphométrie'). We also thank Anthony Herrel for his comments and corrections of this paper. Financial support from the Société d'Anatomie de Paris and the Action Transversale Muséum 'Formes possibles, formes réalisées' of the National Museum of Natural History are gratefully acknowledged.

References

- Baylac M (2010) Rmorph a morphometric library for R. Available from the author: baylac(at)mnhn.fr.
- Bullough P, Goodfellow J, Greenwald AS, et al. (1968) Incongruent surfaces in the human hip joint. *Nature* **217**, 1290.
- Bullough P, Goodfellow J, O'Connor JJ (1973) The relationship between degenerative changes and load-bearing in the human hip. *J Bone Joint Surg Br* **55**, 746–758.
- Byers PD, Contepomi CA, Farkas TA (1970) A post mortem study of the hip joint. Including the prevalence of the features of the right side. *Ann Rheum Dis* **29**, 15–31.
- Calandruccio RA (1987) Arthroplasty of the hip. In: *Campbell's Operative Orthopaedics, Vol. 2* (ed. Crenshaw AH), pp. 1213–1501. St Louis: CV Mosby.
- Dalstra M, Huiskes R (1995) Load transfer across the pelvic bone. *J Biomech* **28**, 715–724.
- Daniel M, Igljic A, Kralj-Igljic V (2005) The shape of acetabular cartilage optimizes hip contact stress distribution. *J Anat* **207**, 85–91.
- Day WH, Swanson SAV, Freeman MAR (1975) Contact pressures in the loaded human cadaver hip. *J Bone Joint Surg Br* **57**, 302–313.
- Fabeck L, Farrok D, Tolley M, et al. (1998) Etude de l'antéversion cotyloïdienne par mesure coxométrique. *J Radiol* **79**, 743–750.
- Fabeck L, Farrok D, Descamps PY, et al. (1999) Etude du recouvrement antérieur de l'acétabulum. *J Radiol* **80**, 1636–1641.
- Ferguson SJ, Bryant JT, Ganz R, et al. (2000a) The acetabular labrum seal: a poroelastic finite element model. *Clin Biomech* **15**, 463–468.
- Ferguson SJ, Bryant JT, Ganz R, et al. (2000b) The influence of the acetabular labrum on hip joint cartilage consolidation: a poroelastic finite element model. *J Biomech* **33**, 953–960.
- Ferguson SJ, Bryant JT, Ganz R, et al. (2003) An in vitro investigation of the acetabular labral seal in hip joint mechanics. *J Biomech* **36**, 171–178.
- Goodfellow J, Bullough P (1968) Studies on age changes in the human hip joint. *J Bone Joint Surg Br* **50**, 222.
- Goodfellow J, Mitsou A (1977) Joint surface incongruity and its maintenance: an experimental study. *J Bone Joint Surg Br* **59**, 446–451.
- Gower JC (1975) Generalized Procrustes Analysis. *Psychometrika* **40**, 33–50.
- Greenwald AS, Haynes DW (1972) Weight-bearing areas in the human hip joint. *J Bone Joint Surg Br* **54**, 157–163.
- Greenwald AS, O'Connor JJ (1971) The transmission of load through the human hip joint. *J Biomech* **4**, 507–512.
- Lazennec JY, Laudet CG, Guérin-Surville H, et al. (1997) Dynamic anatomy of the acetabulum: an experimental approach and surgical implications. *Surg Radiol Anat* **19**, 23–30.
- Lazennec JY, Charlot N, Gorin M, et al. (2004) Hip-spine relationship: a radio-anatomical study for optimization in acetabular cup positioning. *Surg Radiol Anat* **26**, 136–144.
- Lazennec JY, Saillant G (2004) Réflexion sur les rapports entre les hanches et le rachis. *Maitrise Orthop* **130**, <http://www.maitrise-orthop.com/viewPage.do?id=908>.
- Lee YS, Yoon TR (2008) Error in acetabular socket alignment due to the thick anterior pelvic soft tissues. *J Arthropol* **23**, 699–706.
- Lewinnek GE, Lewis JL, Tarr R, et al. (1978) Dislocation after total hip-replacement arthroplasties. *J Bone Joint Surg Am* **60**, 217–220.
- Lewis CL, Sahrman SA (2006) Acetabular labral tears. *Phys Ther* **86**, 110–121.
- Macchiarelli R, Bondioli L, Galichon V, et al. (1999) Hip bone trabecular architecture shows uniquely distinctive locomotor behaviour in South African australopithecines. *J Hum Evol* **36**, 211–323.
- Macchiarelli R, Rook L, Bondioli L (2001) Comparative analysis of the iliac trabecular architecture in extant and fossil primates by mean of digital image processing techniques: implications for the reconstruction of fossil locomotor behaviours. In: *Hominid Evolution and Climatic Change in Europe, Phylogeny of the Neogene Hominoid Primates of Eurasia, Vol. 2* (eds Bonis L, Doufos G, Andrews P), pp. 60–101. Cambridge, UK: Cambridge University Press.
- Martinón-Torres M (2003) Quantifying trabecular orientation in the pelvic cancellous bone of modern humans, chimpanzees, and the Kebara 2 neanderthal. *Am J Hum Biol* **15**, 647–661.
- Maruyama M, Feinberg JR, Capello WN, et al. (2001) Morphologic features of the acetabulum and femur. *Clin Orthop Relat Res* **393**, 52–65.
- Mizrahi J, Solomon L, Kaufman B, et al. (1981) An experimental method for investigating load distribution in the cadaveric human hip. *J Bone Joint Surg Br* **63**, 610–613.
- Murray DW (1993) The definition and measurement of acetabular orientation. *J Bone Joint Surg Br* **75**, 228–232.
- Petersen W, Petersen F, Tillmann B (2003) Structure and vascularisation of the acetabular labrum with regard to pathogenesis and healing of labral lesions. *Arch Orthop Trauma Surg* **123**, 283–288.
- Pinoit Y, May O, Girard J, et al. (2007) Fiabilité limitée du plan pelvien antérieur pour l'implantation assistée par

- informatique de la cupule d'une prothèse totale de hanche. *Rev Chir Orthop* **93**, 455–460.
- R Development Core Team** (2009) *R: A language and Environment for Statistical Computing*. Vienna, Austria: R Foundation for Statistical Computing. ISBN 3-900051-07-0, <http://www.R-project.org>.
- Rholf FJ, Slice DE** (1990) Extensions of the Procrustes method for the optimal superimposition of landmarks. *Syst Zool* **39**, 40–59.
- Richtsmeier JT, Lele SR, Cole TM** (2005) Landmark morphometrics and the analysis of variation. In: *Variation* (eds Hallgrímsson B, Hall BK), pp. 49–68. Boston: Elsevier Academic Press.
- Rousseau MA, Lazennec JY, Boyer P, et al.** (2009) Optimizarion of total hip arthroplasty implantation. Is the anterior pelvic plane concept valid?. *J Arthroplasty* **24**, 22–26.
- Seldes RM, Tan V, Hunt J** (2001) Anatomy, histologic feature, and vascularity of the adult acetabular labrum. *Clin Orthop* **382**, 232–240.
- Shibutani N** (1988) Three-dimensional architecture of the acetabular labrum – a scanning electron microscopic study. *J Jpn Orthop As* **62**, 321–329.
- Slice DE** (2005) *Modern Morphometrics in Physical Anthropology*. Chicago: Kluwer Academic/Plenum.
- Takechi H, Nagashima H, Ito S** (1982) Intra-articular pressure of the hip joint outside and inside the limbus. *J Jpn Orthop As* **56**, 529–536.
- Tan V, Seldes RM, Katz MA** (2001) Contribution of acetabular labrum to articulating surface area and femoral head coverage in adult hip joints: an anatomic study in cadavera. *Am J Orthop* **30**, 809–812.
- Tardieu C, Hecquet J, Barrau A, et al.** (2006) Le bassin, interface articulaire entre rachis et membres inférieurs: analyse par le logiciel De-Visu. *C R Palevol* **5**, 583–595.
- Tardieu C, Hecquet J, Loridon P, et al.** (2008) Deux descripteurs clé des relations sacrocotyloïdienne: les angles d'incidence sacrée et cotyloïde. Mise en évidence par le logiciel De-Visu. *Rev Chir Orthop* **94**, 327–335.
- Teinturier P, Terver S, Jaramillo CV, et al.** (1984) La biomécanique du cotyle. *Rev Chir Orthop* **70**, 41–46.
- Thompson MS, Dawson T, Kuiper JH, et al.** (2000) Acetabular morphology and resurfacing design. *J Biomech* **33**, 1645–1653.
- Vandenbussche E, Saffarini M, Delogé N, et al.** (2007) Hemispheric cups do not reproduce acetabular rim morphology. *Acta Orthop* **78**, 327–332.
- Vandenbussche E, Saffarini M, Taillieu F, et al.** (2008) The asymmetric profile of the acetabulum. *Clin Orthop Relat Res* **466**, 417–423.
- Zilber S, Lazennec JY, Gorin M, et al.** (2004) Variations of caudal, central, and cranial acetabular anteversion according to the tilt of the pelvis. *Surg Radiol Anat* **26**, 462–465.